UNIVERSIDADE D
COIMBRA

Eduardo Borges Matos

SIMULAÇÃO NUMÉRICA DE COMPORTAMENTO MECÂNICO DE NANOTUBOS NÃO CARBÓNICOS

Dissertação no âmbito do Mestrado em Engenharia Mecânica no ramo de Produção e Projeto orientada pela Doutora Nataliya Sakharova e pelo Doutor André Filipe Gomes Pereira apresentada ao Departamento de Engenharia Mecânica da Faculdade de Ciências e Tecnologia da Universidade de Coimbra.

Julho de 2024

1 2 9 0

FACULDADE DE CIÊNCIAS E TECNOLOGIA
UNIVERSIDADE D COIMBRA

Mechanical Behaviour of Non-Carbon Nanotubes: a Numerical simulation study

A dissertation submitted in partial fulfilment of the requirements for the degree of Master in Mechanical Engineering in the speciality of Manufacturing and Design

Simulação numérica de comportamento mecânico de nanotubos não carbónicos

Author

Eduardo Borges Matos

Advisors

Nataliya Sakharova

André Filipe Gomes Pereira

Committee

Chair	**Professor Doutor José Valdemar Birrara Fernandes** **Professor Catedrático da Universidade de Coimbra**
Member[s]	**Professor Doutor Jorge Manuel Afonso Antunes** **Professor Adjunto do Instituto Politécnico de Tomar**
Advisor	**Professora Doutora Nataliya Sakharova** **Investigadora Doutorada da Universidade de Coimbra**

Coimbra, Julho, 2024

“If you can’t fly, run. If you can’t run, walk. If you can’t walk, crawl, but by all means, keep moving.”

Martin Luther King Jr.

ACKNOWLEDGEMENTS

This dissertation would not have been possible without the help of people, who in one way or another, contributed to the preparation and completion of this study.

I could not have undertaken this dissertation without my family and friends whose support help me throughout my academic journey and made this achievement possible.

I would like to express my deepest gratitude to my advisors, Professor Nataliya Sakharova and Professor André Filipe Gomes Pereira, whose guidance, expertise and constructive feedback made this dissertation a possibility.

Abstract

The main objective of the work presented is to perform a numerical simulation study on boron – 15th element group (nitrogen, phosphorus, arsenic and antimony) nanotubes and nanosheets and assess their elastic properties, such as the tensile, bending and torsional rigidities, the Young's and shear moduli, the surface Young's and shear moduli, and Poisson's ratio. To this end a three-dimensional finite element models of single-walled boron nitride, boron phosphide, boron arsenide and boron antimonide nanotubes were built and their elastic properties were evaluated using the nanoscale continuum modelling approach (also called molecular structural mechanics). Afterwards, the numerical results obtained were used to access fitting parameters which allow analytical calculation of the nanotube's elastic properties as a function of nanotube's diameter without the need of the numerical simulation.

The elastic properties (rigidities, Young´s and shear moduli, and Poisson´s ratio) of boron – 15th group nanotubes are discussed with respect to the bond length of the corresponding diatomic hexagonal lattice. The results obtained contribute to a better understanding of the mechanical response of boron compound-based nanotubes.

Keywords: Non-carbon nanotubes, boron – 15th group nanotube, rigidities, elastic moduli, numerical simulation.

Resumo

O objetivo deste trabalho é realizar um estudo de simulação numérica sobre nanotubos e "nanosheets" de boro – Elemento do 15º grupo da tabela periódica (nitrogénio, fosforo, arsénio e antimónio) e avaliar as respetivas propriedades elasticas, tais como rigidezes à tração, flexão e torção, módulos de Young e de corte, módulos de Young e de corte de superfície e coeficiente de Poisson. Para este efeito, foram construídos modelos de elementos finitos tridimensionais de nitreto de boro, fosforeto de boro, arsenieto de boro e antimonieto de boro e as suas propriedades elásticas foram avaliadas utilizando a abordagem de "nanoscale continuum modelling" (também designada por "molecular structural mechanics"). Posteriormente, os resultados numéricos obtidos foram utilizados para obter parâmetros de ajuste que permitem o cálculo analítico das propriedades elásticas do nanotubo em função do seu diâmetro, sem a necessidade de simulação numérica.

As propriedades elásticas (rigidezes, módulos de Young e de cisalhamento, e coeficiente de Poisson) dos nanotubos de boro - Elemento do 15º grupo da tabela periódica são discutidas em função do comprimento de ligação da correspondente matriz hexagonal diatómica. Os resultados obtidos contribuem para uma melhor compreensão da resposta mecânica dos nanotubos à base de compostos de boro.

Palavras-chave: Nanotubos não carbónicos, nanotubos de Boro, rigidezes, módulos de elasticidade, simulação numérica.

Contents

LIST OF FIGURES ix

LIST OF TABLES xi

LIST OF SIMBOLS AND ACRONYMS/ABBREVIATIONS xiii
List of Symbols xiii
Acronyms/Abbreviations xiv

1. INTRODUCTION 1
1.1. Motivation 1
1.2. Key Concepts 2
1.3. Objectives and Dissertation Structure 2

2. LITERATURE REVIEW 5
2.1. Hexagonal boron-based compounds 5
2.2. Modelling approach 5
2.3. Literature Results 6

3. NUMERICAL MODEL 9
3.1. Atomic Structure of Boron – 15th Group Element Nanotubes 9
3.2. Geometrical Characteristics and Finite Element Modelling of the Elastic Behaviour of Single - Walled Boron– 15th Group Element Nanotubes 11
3.3. Elastic Properties of Single - Walled Boron – 15th Group Element Nanotubes 14
3.4. Finite Element Analysis and Elastic Properties of Boron – 15th Group Element Nanosheets 17

4. RESULTS AND DISCUSSION 21
4.1. Rigidities of Boron – 15th group element nanotubes 21
4.2. Elastic Moduli and Poisson's Ratio 24
4.3. Surface Elastic Moduli 28

5. CONCLUSIONS AND FUTURE PERSPECTIVES 33

REFERENCES 35

LIST OF FIGURES

Figure 3.1. BP hexagonal nanosheet with definition of the chiral vector, C_h, chiral indices, n and m, chiral angle, θ, and the schematic to roll up armchair and zigzag geometries. B atoms are depicted in light blue and P are depicted in orange. Adapted from work [16]. 10

Figure 3.2. Structures of (5, 5) armchair, (9, 0) zigzag and (6, 3) chiral of SWBNNTs, SWBPNTs, SWBAsNTs and SWBSbNTs, acquired using Nanotube Modeler© software (version 1.8.0, ©JCrystalSoft, http://www.jcrystal.com). B atoms are depicted in light blue, N atoms are in dark blue, P atoms are in orange, As atoms are in green and Sb atoms are in purple. 13

Figure 3.3. Boundary and loading conditions applied in (a) tension, (b) bending and (c) torsion tests of armchair SWBNNTs. 15

Figure 3.4. Boundary and loading conditions applied in (a) tensile loading in the horizontal direction and (b) tensile loading in the vertical direction for the case of BPNSs. 18

Figure 4.1. Evolution of (a,b) tensile, EA, (c) bending, EI, (e) torsional, GJ, rigidities as a function of NT diameter, D_n; (d) bending, EI, (f) torsional, GJ, rigidities as a function of NT diameter, D_n^3 for SWBNNTs, SWBPNTs, SWBAsNTs, SWBSbNTs in Table 3.2. 22

Figure 4.2. Fitting parameters as a function of bond lengths, $a_{B\text{-}A15}$: (a) $\alpha_{B\text{-}A15}$, (b) $\beta_{B\text{-}A15}$, and $\gamma_{B\text{-}A15}$, for B – A15 nanotubes. 23

Figure 4.3. Evolution of the Young's modulus, E, with the nanotube diameter, D_n, for B – A15 nanotubes and nanosheets 25

Figure 4.4. Evolution of the shear modulus, G, with the nanotube diameter, D_n, for B – A15 nanotubes. 26

Figure 4.5. Evolution of the Poisson's ratio, ν, for B – A15 nanotubes as a function of (a) nanotube diameter, D_n, and (b) bond length, $a_{B\text{-}A15}$ 27

Figure 4.6. Evolution of the surface Young's modulus, E_s, for B – A15 nanotubes and nanosheets as a function of (a) nanotube diameter, D_n, and (b) bond length, $a_{B\text{-}A15}$ 30

Figure 4.7. Evolution of the surface shear modulus, G_s, for B – A15 nanotubes as a function of (a) nanotube diameter, D_n, and (b) bond length, $a_{B\text{-}A15}$. 31

LIST OF TABLES

Table 2.1. Literature results of SWBNNTs and SWBPNTs. 7

Table 3.1. Bond length values of the B-A15 nanotubes [17]. 10

Table 3.2. Chiral indices (n, m) and diameters, D_n, of the single - walled B – A15 nanotubes. 11

Table 3.3. $a_{B\text{-}A15}$, E_s and ν from [17] and calculated values of k_r, k_θ, d and E_b for BN, BP, BAs and BSb nanostructures. 14

Table 3.4. The values of nanotube wall thickness t_n [25]. 16

Table 3.5. Geometry of the B – A15 nanosheets studied. 17

Table 4.1. Fitting parameters $\alpha_{B\text{-}A15}$, $\beta_{B\text{-}A15}$, and $\gamma_{B\text{-}A15}$ for SWBNNTs, SWBPNTs, SWBAsNTs, SWBSbNTs. 23

Table 4.2. Young's and shear moduli, and Poisson's ratio of SWBNNTs, SWBPNTs, SWBAsNTs, SWBSbNTs. 28

Table 4.3. Surface Young's and shear moduli of SWBNNTs, SWBPNTs, SWBAsNTs, SWBSbNTs. 32

LIST OF SIMBOLS AND ACRONYMS/ABBREVIATIONS

List of Symbols

a - unit vector length

$a_{\text{B-A15}}$ - bond length

$\boldsymbol{a_1}$, $\boldsymbol{a_2}$ – unit vectors

A_b – beam element cross section area

$\mathbf{C_h}$ – chiral vector

d – beam element diameter

D_n – nanotube diameter

E – Young's modulus

EA – tensile rigidity

E_b – beam element Young's modulus

EI – bending rigidity

E_s – surface Young's modulus

E_{sx} – nanosheet surface Young's modulus (zigzag configuration)

E_{sy} – nanosheet surface Young's modulus (armchair configuration)

E_x – nanosheet Young's modulus (zigzag configuration)

E_y – nanosheet Young's modulus (armchair configuration)

F_x – nanosheet horizontal axial tensile force

F_y – nanosheet vertical axial tensile force

F_y – nanotube transverse force

F_z – nanotube axial force

G – shear modulus

G_b – beam element shear modulus

GJ – torsional rigidity

G_s – surface shear modulus

I_b – beam element moment of inertia

J_b – beam element polar moment of inertia

k_r – stretching force field constant

k_θ – bending force field constant

k_τ – torsional resistance force field constant

l – beam element length

L_n – nanotube length

L_x – nanosheet horizontal lateral length

L_y – nanosheet vertical lateral length

n, m – chiral indices

T – nanotube torsional moment

t_n – nanotube wall thickness

u_x - nanosheet axial displacement in X axis direction

u_y - nanotube transverse displacement

u_z - nanotube axial displacement

v_y - nanosheet axial displacement in Y axis direction

$\alpha_{B\text{-}A15}$ - tensile rigidity fitting parameter

$\beta_{B\text{-}A15}$ - bending rigidity fitting parameter

$\gamma_{B\text{-}A15}$ - torsional rigidity fitting parameter

θ – chiral angle

ν – Poisson's Ratio

φ - nanotube twist angle

Acronyms/Abbreviations

1D – One-Dimensional

2D – Two-Dimensional

3D – Three-Dimensional

As – Arsenic

B – Boron

B-A15 – Boron – 15th element group

BAsNSs – Boron Arsenide Nanosheets

BNNSs – Boron Nitride Nanosheets

BPNSs – Boron Phosphide Nanosheets

BSbNSs – Boron Antimonide Nanosheets

CM – Continuum Mechanics

CNTs – Carbon Nanotubes

DFT – Density Functional Theory

FE – Finite Element

FEA – Finite Element Analysis

h-BAs – Hexagonal Boron Arsenide

h-BN – Hexagonal Boron Nitride

h-BP – Hexagonal Boron Phosphide

MM – Molecular Mechanics

N – Nitrogen

NCM/MSM – Nanoscale Continuum Modelling / Molecular Structural Mechanics

N-CNTs – Non-carbon Nanotubes

NSs – Nanosheets

NTs – Nanotubes

P – Phosphorus

Sb - Antimony

SWBAsNTs – Single Walled Boron Arsenide Nanotubes

SWBNNTs – Single Walled Boron Nitride Nanotubes

SWBPNTs – Single Walled Boron Phosphide Nanotubes

SWBSbNTs – Single Walled Boron Antimonide Nanotubes

UFF – Universal Force Field

vdW – van der Walls

1. INTRODUCTION

This opening chapter introduces the motivation behind this dissertation, presents fundamental ideas for a better understanding of the study carried out in this work as well as its objectives and a brief summary of what is covered in each chapter.

1.1. Motivation

The remarkable properties of carbon nanotubes (CNTs) and their multiple potential applications allowed them to become the most widely researched nanostructures which then spurred studies to predict new cylindrical structures with a honeycomb diatomic arrangement. These nanostructures, i.e. nanotubes, based on elements different from carbon and their compounds, have graphene-like lattice and are designated as non-carbon nanotubes (N-CNTs).

The N-CNTs are emerging materials with more promising optical, thermal and electrical properties when compared with the CNTs. Which in turn lead to a growing interest in their technological use. Non-carbon nanotubes are attractive for electronic engineering and light industry, they can be a potential base for the construction of nanosystems and nanodevices. Moreover, the mechanical stability of the N-CNTs and the knowledge on their mechanical behaviour are crucial for the design of materials and instrument. However, a well-known lack of numerical and experimental studies on the mechanical properties of N-CNTs makes difficult to take full advantage of the N-CNTs in current and forthcoming technological applications. This dissertation aims to fill this gap.

For this objective the compounds in focus will be those formed by the elements of the 15th group of the periodic table, such as nitrogen (N), phosphorus (P), arsenic (As) and antimony (Sb) which are able to establish honeycomb diatomic arrangement with boron (B), resulting in the following nanotubes (NTs), boron nitride nanotubes (BNNTs), boron phosphide nanotubes (BPNTs), boron arsenide nanotubes (BAsNTs) and boron antimonide nanotubes (BSbNTs).

Amongst selected nanotubes, BNNTs are the most widely studied, while the other NTs have not received the same research attention to date, especially BAsNTs and BSbNTs, for which a lack of studies regarding their mechanical properties is noticeable.

In this context the objective of this work is to perform a systematic comparative study on the evaluation of the elastic and surface elastic (Young´s and shear) moduli, and Poisson´s ratio of single-walled nanotubes composed by boron nitride, boron phosphide, boron arsenide and boron antimonide (SWBNNTs, SWBPNTs, SWBAsNTs and SWBSbNTs) in a wide range of chiral indices and diameters. The results envisage unlocking new perspectives for the use boron – 15th group element nanotubes in innovative devices and their accurate design and robust performance.

1.2. Key Concepts

Since experimental procedures are costly and resource intensive, the present study on the mechanical behaviour of N-CNTs is carried out numerically, resorting to the nanoscale continuum modelling (NCM) also called molecular structural mechanics (MSM) approach. The NCM/MSM approach is the most commonly indicated for effective and fast simulation of N-CNTs mechanical response.

This approach makes use of the linking between the nanotube molecular structure and the equivalent continuum structure, modelling bonds between two atoms in the diatomic structure as beam elements. The force-field constants, representing the NT molecular structure, are used to deduce the geometric and elastic properties of the beams, which in their turn are employed as input parameters for the finite element (FE) simulation. A three-dimensional numerical model of the boron – 15th group nanotubes is built, which allows determining their tensile, bending and torsional rigidities, and subsequently calculating their Young´s and shear moduli, and the Poisson ratio.

1.3. Objectives and Dissertation Structure

The main objectives of this dissertation are to assess the elastic properties of the boron – 15th group nanotubes in a wide range of chiral indices and diameters. As such this dissertation can be divided in 5 different chapter:

- In Chapter 1 the motivation behind this dissertation as well key concepts necessary to understanding of the current study are explained. Finally, the objectives and dissertation structure are presented:

- In Chapter 2 a brief review of the literature is presented as along with the results from literature regarding the nanotubes under study;
- In Chapter 3 the numerical model is explained and its input parameters (the geometrical and elastic properties of beam elements) are defined;
- In Chapter 4 the results of the finite element analysis (FEA) are presented along with calculated values of the elastic properties of the boron - 15^{th} group element nanotubes and nanosheets;
- In Chapter 5 a brief summary of the main findings of this dissertation and perspectives of future work are presented.

2. LITERATURE REVIEW

This chapter aims to review the literature review and explore selected results that are aligned with in the scope of this dissertation.

2.1. Hexagonal boron-based compounds

Hexagonal boron nitride (h-BN) is a high strength electric insulator, comparable to graphene, excellent thermal and chemical stability, and transparency for visible light [1]. Such characteristics make h-BN suitable for diverse applications as a dielectric in graphene electronics, components for photovoltaic devices, sensors and bio-detectors.

Other 2D hexagonal compounds containing boron, such as semiconducting hexagonal boron phosphide (h-BP), with an appropriate band gap (0.82–1.81 eV) might be experimentally challenging but could bring some opportunities in the applications of electronic devices even more spectacular that can operate in hazard environments (high temperature or intense radiation). The h-BP monolayer has been of great interest for researchers who demonstrate that it is a direct band gap semiconductor with potential application as field effect transistors [2].

Hexagonal boron arsenide (h-BAs) is attracting research interest as an extremely promising material for modern electronics and optoelectronic devices since it is the only known semiconducting with ultrahigh thermal conductivity of 2000 W/m·K at room temperature, enabling it to rapidly dissipate the heat loads. It also has potential as gas sensor for detecting SO_2 gas molecules [3].

One-dimensional (1D) tubular nanostructures, i.e. nanotubes (NTs), made up from hexagonal BN, BP, BAs, and BSb monolayers, are expected to have enhanced properties when compared with their bulk counterparts, envisioning new perspectives in the development of nanoscale electronic and light devices, but not limited to them.

2.2. Modelling approach

As previously mentioned, the NCM/MSM approach explores the connection between molecular configuration of the nanotube and the solid mechanics and considers the bonds between two atoms in the diatomic structure as beam elements.

Extensive research has focused on single-walled boron nitride nanotubes (SWBNNTs), the works [4], [5], [6], [7], studied the elastic (elastic moduli and Poisson's ratio) and dynamic (vibrational) properties, electromechanical properties, and size dependent elastic properties basing on the NCM/MSM method and using beam elements to replace the B-N bond. In the study [8] a representative cell with a boron atom connected to three nitride atoms by covalent bonds was utilized. Meanwhile in the work [9] the NCM/MSM and CM (Continuum Mechanics) approaches were combined to determine the Young's and shear moduli, and Poisson's ratio of SWBNNTs by linking the "stick-and-spring" model to the continuum thin shell Donnell models. The authors of the study [10] proposed closed-formed analytical solutions based on the "stick-and-spring" model, to investigate the buckling behaviour and assess the surface Young's modulus and Poisson's ratio.

A critical aspect of the NCM/MSM approach is the accurate determination of the force field constants, bond stretching and bending, k_r and k_θ, respectively, which are required for calculating the geometrical and elastic properties of the beam elements representing the interatomic bonds. Among the most well-established and commonly used methods for calculating the force field constants include those based on Universal Force Field (UFF) [11], DREIDING force field [12] and ab initio density functional theory (DFT) computations, combined with analytical expressions resulting from molecular mechanics (MM).

2.3. Literature Results

In Table 2.1 are shown relevant literature results obtained basing on the NCM/MSM approach. As can be seen, the elastic properties results are almost all for the SWBNNTs with the exception of two studies, where the results for single-walled boron phosphide nanotubes (SWBPNTs) can be found. For the cases of single-walled boron arsenide and boron antimonide nanotubes (SWBAsNTs and SWBSbNTs) to the best of our knowledge the studies towards their elastic properties are non-existent.

Table 2.1. Literature results of SWBNNTs and SWBPNTs.

Year	Reference	Method	NTs type*		E, TPa	G, TPa	ν	E_s, TPa*nm**	G_s, TPa*nm**
2006	[4]	Beams + FE models	BN	(n,n) (n,0)	0.960 0.975	0.465 0.475	-	-	
2011	[13]	"stick-and-spring" model + closed form solution	BN	(n,n) (n,0)	-	-	-	0.270 0.262	0.095 0.088
2015	[6]	Analytical solution	BN	(n,n) (n,0)	0.825 0.823	-	0.217	-	
2015	[8]	Representative cell	BN	(n,n) (n,0)	0.970 0.967	0.416 0.418	-	-	
2016	[10]	"stick-and-spring" model + analytical	BN BP	(n,n) (n,0) (n,n) (n,0)	-	-	0.216 0.219 0.360 0.365	0.278 0.276 0.118 0.117	
2018	[5]	Beams + FE models	BN	(n,n) (n,0)	0.928	-	-	-	
2019	[14]	Longitudinal and torsional vibrations	BN	(n,n) (n,0) (n,m)	0.972	0.418	-	-	
2019	[9]	"stick-and-spring" model + Donnel thin shell model	BN	(n,n) (n,0)	-	-	0.239 0.226	0.255 0.250	0.092 0.104
2021	[7]	Beams + FE models	BN	(n,n) (n,0)	0.984	0.486	0.150	-	–

				(n,m)					
2022	[15]	Beams + FE models	BP	(n,n) (n,0) (n,m)	-	-	0.060	0.176	0.083
2024	[16]	Beams + FE models	BN	(n,n) (n,0) (n,m)	-	-	0.01	0.329	0.163

* All theoretical results presented were obtained for single-walled NTs.

** The surface Young's ($E_S = Et_n$) and shear ($G_S = Gt_n$) moduli, where t_n is the nanotube wall thickness.

3. NUMERICAL MODEL

In this chapter the three-dimensional (3D) finite element model used to carry out the finite element analysis (FEA) is presented, as well as the parameters necessary for the numerical simulation.

3.1. Atomic Structure of Boron – 15th Group Element Nanotubes

As mentioned previously the nanotubes under study are composed of an atom of the 15th group of the periodic table, such as nitrogen (N), phosphorus (P), arsenic (As) and antimony (Sb), which hereinafter referred as A15, which form with boron (B) into a honeycomb structure. The hexagonal lattice of the different boron compounds has planar geometry [17] as shown in Figure 3.1 for the case of BP nanosheet. The honeycomb atomic arrangement is defined by the chiral vector, $\mathbf{C_h}$, and chiral angle, θ, expressed by the following equations (1) and (2), respectively, [18], [19]:

$$\mathbf{C_h} = \mathrm{n}\boldsymbol{a_1} + \mathrm{m}\boldsymbol{a_2} \quad (1),$$

$$\theta = \sin^{-1}\frac{\sqrt{3}}{2}\frac{\mathrm{m}}{\sqrt{\mathrm{n}^2 + \mathrm{nm} + \mathrm{m}^2}} \quad (2),$$

where n and m, the chiral indices, have integers values; $\boldsymbol{a_1}$ and $\boldsymbol{a_2}$ are the unit vectors of the hexagonal lattice. The length of the unit vector a is calculated by following expression[20]:

$$a = \sqrt{3}a_{\mathrm{B-A15}} \quad (3),$$

where $a_{\text{B-A15}}$ is the equilibrium bond length. The values of the bond lengths of the B-A15 nanotubes used in this dissertation are presented below in Table 3.1.

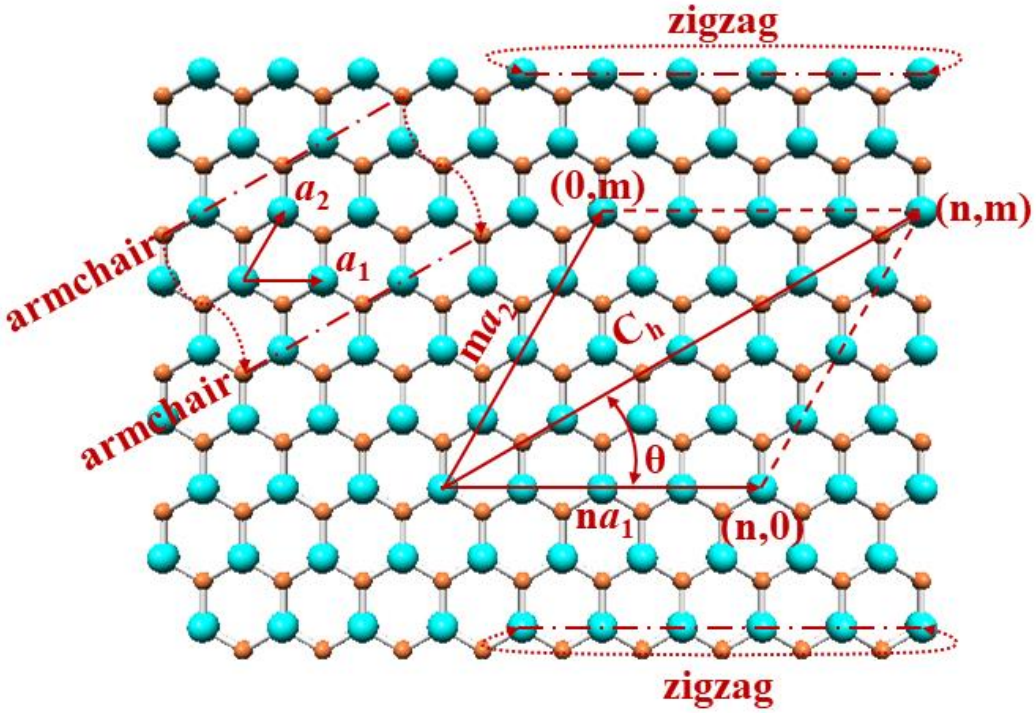

Figure 3.1. BP hexagonal nanosheet with definition of the chiral vector, $\mathbf{C_h}$, chiral indices, n and m, chiral angle, θ, and the schematic to roll up armchair and zigzag geometries. B atoms are depicted in light blue and P are depicted in orange. Adapted from work [16].

Table 3.1. Bond length values of the B-A15 nanotubes [17].

	BN	**BP**	**BAs**	**BSb**
$a_{\text{B-A15}}$, **nm**	0.145	0.183	0.193	0.212

The B-A15 nanosheets can be rolled up into a cylinder in different ways to form the single walled nanotubes, resulting in three nanotube symmetry groups depending on the chiral angle, θ, as can be seen in Figure 3.1. The value of θ is varied between 0º, when m=0, for zigzag (n,0) and 30º, when n=m, for armchair (n, n), which are called the non-chiral nanotubes. The remaining cases where $0º<\theta<30º$ ($n\neq m\neq 0$) are designated as chiral nanotubes. The diameter of the resulting nanotube, D_n, is given by equation (4)[21]:

$$D_n = \frac{a_{B-A15}\sqrt{3(n^2+nm+m^2)}}{\pi} \quad (4)$$

3.2. Geometrical Characteristics and Finite Element Modelling of the Elastic Behaviour of Single - Walled Boron– 15th Group Element Nanotubes

In Table 3.2 the geometric characteristics of the different single-walled B – A15 nanotubes, used in the finite element analysis (FEA), are shown in their three main configurations, armchair ($\theta = 30^o$), zigzag ($\theta = 0^o$) and chiral ($\theta = 19.1^o$ family, which is consistent with the biggest number of NTs). The selection of the chiral indices was made with the goal of obtaining NTs with similar diameters which have an aspect ratio of approximately 30:1 (length: diameter) to guarantee the mechanical response regardless of the NTs length.

Table 3.2. Chiral indices (n, m) and diameters, D_n, of the single - walled B – A15 nanotubes.

NT Type	SWBNNTs		SWBPNTs		SWBAsNTs		SWBSbNTs	
	(n, m)	D_n, nm*	(n, m)	D_n, nm	(n, m)	D_n, nm	(n, m)	D_n, nm
Armchair, θ = 30º	(4, 4)	0.561	(3, 3)	0.524	(3, 3)	0.553	(3, 3)	0.607
	(6, 6)	0.842	(5, 5)	0.874	(5, 5)	0.922	(4, 4)	0.810
	(9, 9)	1.263	(7, 7)	1.223	(7, 7)	1.290	(6, 6)	1.215
	(12, 12)	1.684	(9, 9)	1.573	(9, 9)	1.659	(8, 8)	1.620
	(16, 16)	2.246	(13, 13)	2.272	(12, 12)	2.212	(11, 11)	2.227
	(22, 22)	3.088	(18, 18)	3.146	(17, 17)	3.133	(15, 15)	3.037
	(29, 29)	4.071	(23, 23)	4.019	(22, 22)	4.055	(20, 20)	4.049
Zigzag, θ = 0º	(9, 0)	0.729	(7, 0)	0.706	(7, 0)	0.745	(6, 0)	0.701
	(14, 0)	1.135	(11, 0)	1.110	(11, 0)	1.170	(10, 0)	1.169
	(19, 0)	1.540	(15, 0)	1.513	(14, 0)	1.490	(13, 0)	1.519
	(23, 0)	1.864	(18, 0)	1.816	(17, 0)	1.809	(16, 0)	1.870
	(31, 0)	2.512	(24, 0)	2.421	(23, 0)	2.447	(21, 0)	2.455
	(43, 0)	3.485	(34, 0)	3.430	(32, 0)	3.405	(29, 0)	3.390
	(49, 0)	3.971	(39, 0)	3.935	(37, 0)	3.937	(34, 0)	3.974
Chiral, θ = 19.1º	(6, 3)	0.643	(4, 2)	0.534	(4, 2)	0.563	(4, 2)	0.618
	(10, 5)	1.072	(8, 4)	1.068	(8, 4)	1.126	(6, 3)	0.928
	(16, 8)	1.715	(12, 6)	1.602	(12, 6)	1.689	(12, 6)	1.855
	(20, 10)	2.144	(16, 8)	2.136	(14, 7)	1.971	(14, 7)	2.165
	(26, 13)	2.788	(20, 10)	2.669	(20, 10)	2.815	(18, 9)	2.783
	(34, 17)	3.645	(28, 14)	3.737	(26, 13)	3.660	(24, 12)	3.711
	(40, 20)	4.289	(32, 16)	4.271	(30, 15)	4.223	(28, 14)	4.329

* The diameters, D_n, of SWBNNTs are calculated adopting the bond lengths $a_{B\text{-}N}$= 0.147 nm, as defined by Nanotube Modeler©software.

The FE meshes of SWBNNTs, SWBPNTs, SWBAsNTs and SWBSbNTs used in the FEA were built using the Nanotube Modeler© software. The program database files obtained needed to be converted to a format supported by ABAQUS® code (Abaqus 2020, Dassault Systèmes®). To this purpose the in-house program InterfaceNanotubes.NM was used [7]. Nanotube structures for armchair, zigzag and chiral nanotubes based on the boron compounds are exemplified in Figure 3.2.

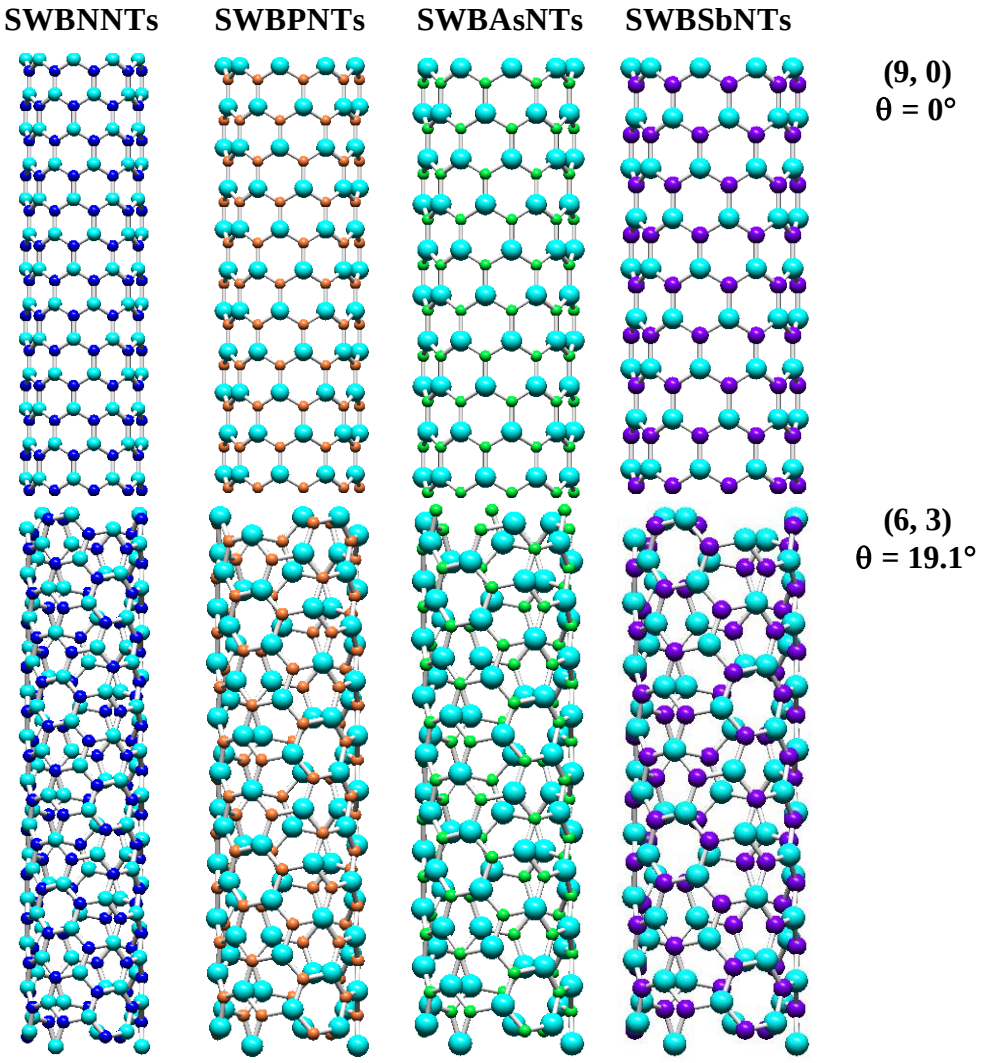

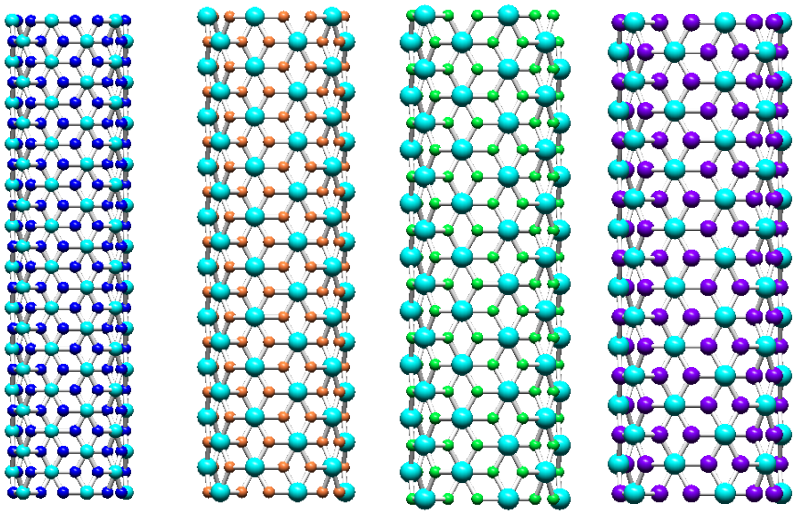

Figure 3.2. Structures of (5, 5) armchair, (9, 0) zigzag and (6, 3) chiral of SWBNNTs, SWBPNTs, SWBAsNTs and SWBSbNTs, acquired using Nanotube Modeler© software (version 1.8.0, ©JCrystalSoft, http://www.jcrystal.com). B atoms are depicted in light blue, N atoms are in dark blue, P atoms are in orange, As atoms are in green and Sb atoms are in purple.

The interatomic bonds, B-A15 of the hexagonal diatomic lattice, were modelled as equivalent beam elements within the NCM/MSM method, which makes use of the linkage between the nanotube molecular structure and the equivalent continuum structure. The equivalent continuum structure, composed of beam elements, is characterised by the tensile, E_bA_b, bending, E_bI_b, and torsional, G_bJ_b, rigidities of beams, which are related to the bond stretching, k_r, bending, k_θ, and torsional resistance, k_τ, force field constants, representing respective molecular NT structure, as expressed by equation (5) shown below [22]:

$$E_bA_b = lk_r, E_bI_b = lk_\theta, G_bJ_b = lk_\tau \tag{5}$$

where $A_b = \pi d^2/4$ is the cross-section area, $I_b = \pi d^4/64$ is the moment of inertia, and $J_b = \pi d^4/32$ is the polar moment of inertia of a circular cross-section beam with diameter d and being l the beam length, equivalent to bond length, $a_{B\text{-}A15}$.

Using equation (5) the computation of the numerical simulation input parameters is now possible utilising the force field constants, k_r and k_θ which for most of the B – A15 NTs, except BNNTs are either scarce or non-existent. Therefore, in this dissertation, the k_r and k_θ force field constants were calculated using equations, respectively [16]:

$$k_r = \frac{3E_s}{\sqrt{3}(1-\nu)} \tag{6}$$

$$k_\theta = \frac{E_s a_{B-A15}^2}{2\sqrt{3}(1+3\nu)} \quad (7)$$

The values of the surface Young's modulus, E_s, and the Poisson's ratio, ν, in turn, originate from DFT calculations or can be obtained experimentally.

Combining equations (6) and (7) with equation (5) it is possible to calculate the geometrical (diameter) and elastic (Young's modulus) properties of the beam, d and E_b, respectively, which used as input in the numerical simulation, as follows:

$$d = 4\sqrt{k_\theta / k_r} \quad (8)$$

$$E_b = \frac{k_r^2 l}{4\pi k_\theta} \quad (9)$$

where $a_{B-A15} = l$ is the beam length.

The parameters a_{B-A13}, E_s and ν, necessary for calculating the bond stretching, k_r, and bending, k_θ, force constants (Equations (6) and (7)) together with calculated k_r and k_θ values are shown in Table 3.3.

Table 3.3. $a_{B\text{-}A15}$, E_s and ν from [17] and calculated values of k_r, k_θ, d and E_b for BN, BP, BAs and BSb nanostructures.

Compound	$a_{B\text{-}A15}$, nm	E_s, nN/nm	ν	k_r, nN/nm	k_θ, nN · nm/rad^2	d, nm	E_b, GPa
BN	0.145	267	0.21	585	0.994	0.165	3977
BP	0.183	135	0.28	325	0.709	0.187	2165
BAs	0.193	119	0.29	290	0.684	0.194	1892
BSb	0.212	91	0.34	239	0.584	0.198	1646

3.3. Elastic Properties of Single - Walled Boron – 15th Group Element Nanotubes

The first elastic properties of the B – A15 nanotubes determined were the tensile, EA, bending, EI, and torsional, GJ, rigidities which were obtained from the results of the FEA, simulating tensile, bending and torsion tests with help of the ABAQUS® FE code. The boundary and loading conditions applied in these tests are shown in Figure 3.3. For tensile, bending and torsion tests, the axial force, F_z, the transverse force, F_y, and the torsional moment, T, respectively, were applied to one end of the nanotube, while on the opposite end the boundary conditions restricting all degrees of freedom of the edge nodes were applied.

In the torsion test, one more boundary condition is needed to be applied, which restricted the radial movement of the edge nodes, as shown in Figure 3.3c. As a result of the tensile, bending and torsion tests carried out it is possible to obtain the axial, u_z, and transverse, u_y, displacements and the twist angle, φ, respectively, directly from the FEA. Using these values, the tensile, EA, bending, EI, and torsional, GJ, rigidities of the B – A15 nanotube with length L_n are calculated as follows:

$$EA = \frac{F_z L_n}{u_z} \tag{10}$$

$$EI = \frac{F_y L_n}{3u_y} \tag{11}$$

$$GJ = \frac{T L_n}{\varphi} \tag{12}$$

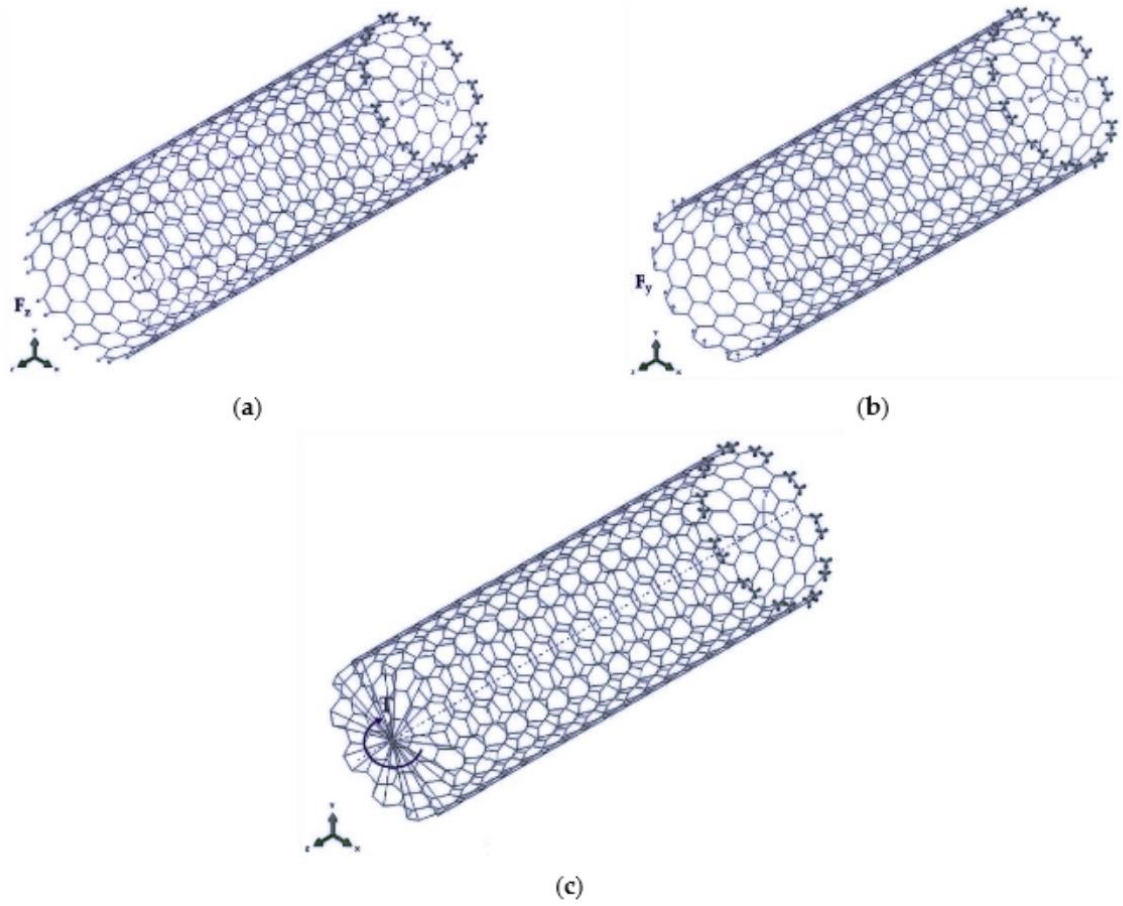

Figure 3.3. Boundary and loading conditions applied in (a) tension, (b) bending and (c) torsion tests of armchair SWBNNTs.

After determining the tensile, EA, bending, EI, and torsional, GJ, rigidities, it is now possible to calculate the Young's and shear moduli, E and G, respectively, and the Poisson's ratio, respectively, by the following expressions [23], [24]:

$$E = \frac{EA}{\pi t_n \sqrt{8\left(\frac{EI}{EA}\right) - t_n^2}} \tag{13}$$

$$G = \frac{GJ}{2\pi t_n \left(\frac{EI}{EA}\right)\sqrt{8\left(\frac{EI}{EA}\right) - t_n^2}} \tag{14}$$

$$\nu = \frac{E}{2G} - 1 = \frac{EI}{GJ} - 1 \tag{15}$$

where t_n is the nanotube wall thickness. The values of t_n of are rare for most of the B – A15 nanotubes, except for BNNTs, so the t_n values, equal to the van der Waals (vdW) diameter [25] were used as shown in Table 3.4.

Table 3.4. The values of nanotube wall thickness t_n [25].

Compound	t_n, nm
BN	0.340
BP	0.372
BAs	0.377
BSb	0.398

Considering the uncertainty of the values of NTs wall thickness, the surface elastic moduli, Young's ($E_s = Et_n$) and shear ($G_{Ss} = Gt_n$) moduli, are evaluated as they are more reliable to describe the mechanical response of the NTs since the surface elastic moduli do not depend on t_n. Taking into account that $t_n^2 \ll 8\,(EI/EA)$ and the term t_n^2 in equations (13) and (14) can be neglected, the surface Young's, E_s, and shear, G_s, moduli are determined, respectively, as follows:

$$E_S = Et_n = \frac{EA}{\pi\sqrt{8\left(\frac{EI}{EA}\right)}} \tag{16}$$

$$G_S = Gt_n = \frac{GJ}{2\pi\left(\frac{EI}{EA}\right)\sqrt{8\left(\frac{EI}{EA}\right)}} \tag{17}$$

3.4. Finite Element Analysis and Elastic Properties of Boron – 15th Group Element Nanosheets

In addition to studying the elastic properties of the B – A15 nanotubes, the elastic response of the respective nanosheets (NSs) was studied and their Young's moduli were assessed. To this end, the geometric properties of the B – A15 nanosheets, shown in Table 3.5, were chosen such that the vertical and horizontal lateral lengths, L_y and L_x, respectively, were approximately the same, maintaining an aspect ratio of 1:1, obtaining a square in the range of 15×15 nm^2.

Table 3.5. Geometry of the B – A15 nanosheets studied.

Compound	L_x, nm	L_y, nm	Aspect Ratio, L_y:L_x	Number of Elements	Number of Nodes
BN	15.276	15.729	1:1	12936	8712
BP	15.215	15.738	1:1	8333	5626
BAs	16.045	16.598	1:1	8333	5626
BSb	15.790	15.688	1:1	6432	4350

Following a similar approach to the nanotubes under study, the FE meshes of boron nitride nanosheets (BNNSs), boron phosphide nanosheets (BPNSs), boron arsenide nanosheets (BAsNSs) and boron antimonide nanosheets (BSbNSs) to be used in the FEA were built aiding the Nanotube Modeler© software. Subsequently the program database files were converted to a format supported by ABAQUS® code (Abaqus 2020, Dassault Systèmes®) using the in-house program InterfaceNanotubes.NM [7].

In the ABAQUS® FE code the mechanical response of the B – A15 nanosheets was studied under numerical tensile tests, as shown in Figure 3.4. In the first loading case depicted in Figure 3.4a, the edge nodes on the left side of the nanosheet were fixed, and the horizontal axial tensile force, F_x, was applied on the nodes of the opposite (right) side of the nanosheet. Similarly, in Figure 3.4b, the edge nodes on the bottom side were fixed and the vertical axial tensile, F_y, force was applied to the nodes on the upper side of the nanosheet. The abovementioned loading conditions mean that two tensile configurations of the B – A15 nanosheets, zigzag and armchair, respectively, are considered.

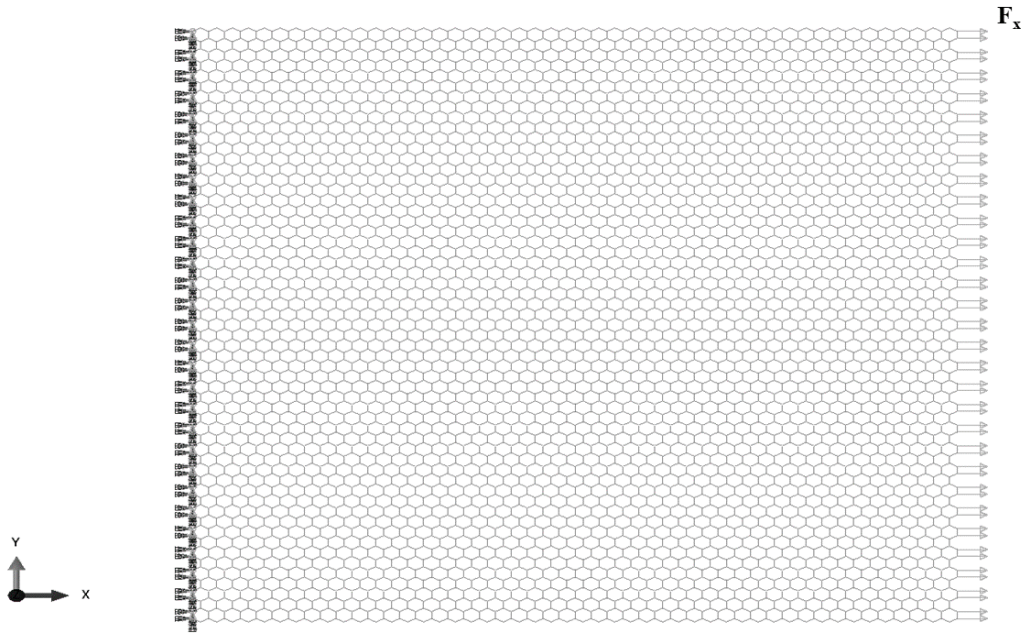

(a)

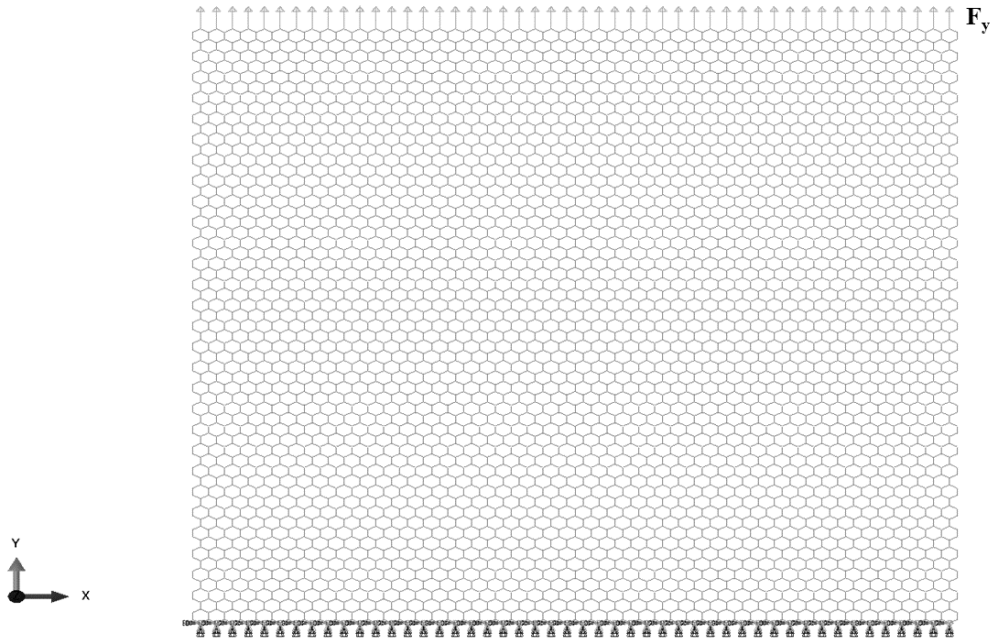

(b)

Figure 3.4. Boundary and loading conditions applied in (a) tensile loading in the horizontal direction and (b) tensile loading in the vertical direction for the case of BPNSs.

To calculate the Young´s moduli along the x and y axes, E_x and E_y, respectively, the axial displacements of the nanosheet in the x, u_x, and in the y, v_y, directions under the applied forces, F_x and F_y, respectively, were taken from the FEA and evaluated as follows [26]:

$$E_x = \frac{F_x L_x}{u_x L_y t_n} \tag{18}$$

$$E_y = \frac{F_y L_y}{v_y L_x t_n} \tag{19}$$

where L_x and L_y are the nanosheet side lengths, and t_n the nanosheet thickness.

Given the uncertainty or lack thereof the values the nanosheet thickness, the alternative to E_x and E_y is to calculate the surface Young's moduli in zigzag, E_{sx}, and armchair, E_{sy}, directions, as follows [26]:

$$E_{sx} = E_x t_n = \frac{F_x L_x}{u_x L_y} \tag{20}$$

$$E_{sy} = E_y t_n = \frac{F_y L_y}{v_y L_x} \tag{21}$$

4. RESULTS AND DISCUSSION

In this chapter the results of the FEA along with the calculated values of the elastic properties of the nanotubes and nanosheets formed by boron compounds are presented.

4.1. Rigidities of Boron – 15th group element nanotubes

The tensile, bending and torsional (EA, EI and GJ, respectively) rigidities of the single walled B – A15 nanotubes, calculated by equations (10), (11) and (12), using the results obtained from the FEA, are plotted as a function of the nanotube diameter D_n in Figure 4.1a,c,e. For each of the three rigidities, their values increase with the increase of the nanotube diameter, regardless of the nanotube compound or symmetry group (armchair, zigzag and chiral), and decrease from the values obtained for SWBNNTs to SWBSbNTs. As shown in other authors' works[15], [27], [28], in the case of the B – A15 nanotubes, the tensile rigidity, EA, can be described by a linear function of D_n (Figure 4.1b), while the bending and torsional rigidities can be described by a linear function of D_n^3 (Figure 4.1d,f). The slope of the straight lines in Figure 4.1b,d,f can be determined as follows [23]:

$$EA = \alpha_{B-A15} D_n \tag{22}$$

$$EI = \beta_{B-A15} D_n^3 \tag{23}$$

$$GJ = \gamma_{B-A15} D_n^3 \tag{24}$$

In these equations, α_{B-A15}, β_{B-A15}, and γ_{B-A15} are fitting parameters, and D_n is the nanotube diameter. These parameters' values are obtained from the slope of the dashed lines in Figure 4.1b,d,f, with the R-squared values always being better than 0.9999, regardless of the rigidity and compound forming the nanotubes. The α_{B-A15}, β_{B-A15}, and γ_{B-A15} fitting parameters are shown in Table 4.1.

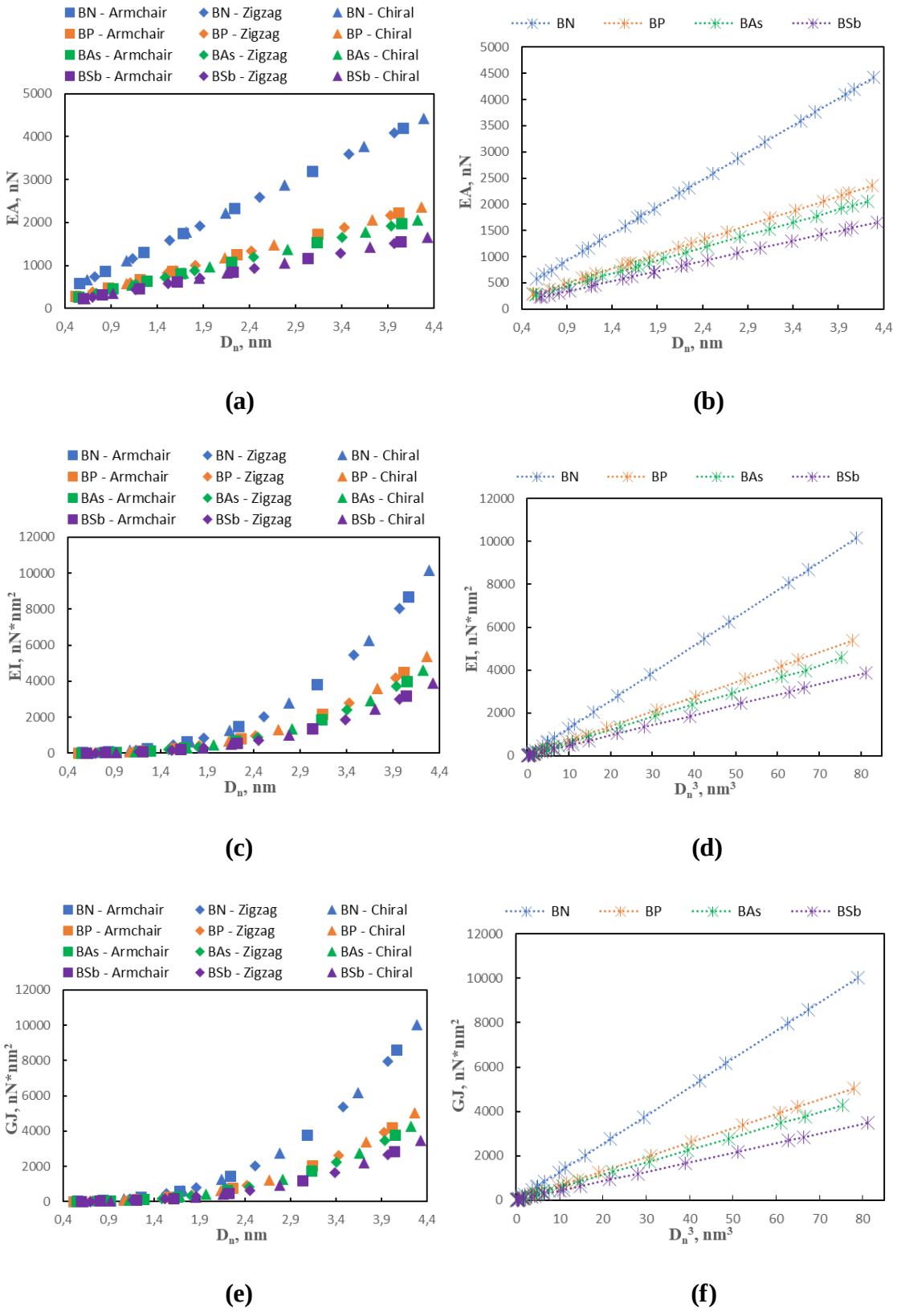

Figure 4.1. Evolution of (**a,b**) tensile, EA, (**c**) bending, EI, (**e**) torsional, GJ, rigidities as a function of NT diameter, D_n; (**d**) bending, EI, (**f**) torsional, GJ, rigidities as a function of NT diameter, D_n^3 for SWBNNTs, SWBPNTs, SWBAsNTs, SWBSbNTs in Table 3.2.

Table 4.1. Fitting parameters $\alpha_{\text{B-A15}}$, $\beta_{\text{B-A15}}$, and $\gamma_{\text{B-A15}}$ for SWBNNTs, SWBPNTs, SWBAsNTs, SWBSbNTs.

Compound	Fitting Parameters		
	$\alpha_{\text{B-A15}}$, nN/nm	$\beta_{\text{B-A15}}$, nN/nm	$\gamma_{\text{B-A15}}$, nN/nm
BN	1031.04	128.77	127.06
BP	551.04	68.84	64.75
BAs	486.87	60.45	56.70
BSb	381.70	47.69	42.74

The fitting parameters α_{B-A15}, β_{B-A15}, and γ_{B-A15} allow the quantification of the tensile, bending and torsional rigidities, respectively, thereby describing the mechanical response of nanotubes when subjected to tension, bending and torsion. For this purpose, the values of α_{B-A15}, β_{B-A15} and γ_{B-A15} are presented in Figure 4.2, for the bond lengths, a_{B-A15}, corresponding to SWBNNTs, SWBPNTs, SWBAsNTs, SWBSbNTs, where we can see all three fitting parameters drop from SWBNNTs to SWBPNTs and then gradually decrease until SWBSbNTs, as the bond length value increases. It can be concluded that the major factor which influences the value of the rigidities of the B – A15 nanotubes is the bond length, a_{B-A15}. As we can see that as this value increases, the tensile, EA, bending, EI, and torsional, GJ, rigidities decrease.

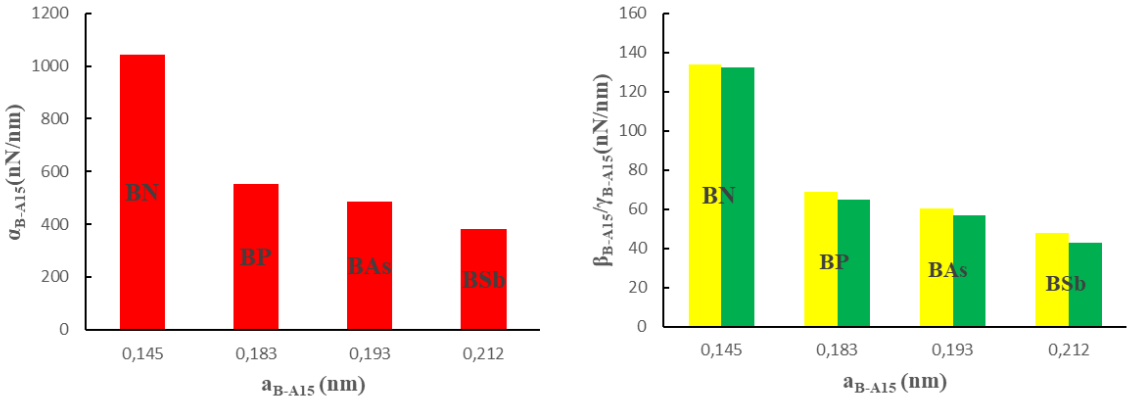

(a) **(b)**

Figure 4.2. Fitting parameters as a function of bond lengths, $a_{\text{B-A15}}$: **(a)** $\alpha_{\text{B-A15}}$, **(b)** $\beta_{\text{B-A15}}$, and $\gamma_{\text{B-A15}}$, for B – A15 nanotubes.

4.2. Elastic Moduli and Poisson's Ratio

In this section, the Young's and shear moduli and the Poisson's ratio of the SWBNNTs, SWBPNTs, SWBAsNTs and SWBSbNTs, calculated by equations (13)-(15), using the rigidities obtained by the FEA, respectively, are analysed. However, it should be noted that by using the fitting parameters α_{B-A15}, β_{B-A15}, and γ_{B-A15}, presented in Table 4.1, and the values of the nanotube diameter, D_n, and wall thickness, t_n, and linking equations (13)-(15) with equations (22)-(24), the Young's and shear moduli and the Poisson's ratio can be calculated without resorting to the FEA results, respectively, as follows [7]:

$$E = \frac{\alpha_{B-A15} D_n}{\pi t_n \sqrt{8\left(\frac{\beta_{B-A15}}{\alpha_{B-A15}}\right) D_n^2 - t_n^2}} \tag{25}$$

$$G = \frac{\gamma_{B-A15} D_n}{2\pi\left(\frac{\beta_{B-A15}}{\alpha_{B-A15}}\right) t_n \sqrt{8\left(\frac{\beta_{B-A15}}{\alpha_{B-A15}}\right) D_n^2 - t_n^2}} \tag{26}$$

$$\nu = \frac{\beta_{B-A15}}{\gamma_{B-A15}} - 1 \tag{27}$$

In Figure 4.3 the evolution of the Young's modulus, E, with the nanotube diameter, D_n, as well as the values calculated by equation (25) are shown. Regardless of compound or chirality, the Young's modulus at the beginning decreases with nanotube diameter, until it reaches diameters $D_n > 1.9$ nm, where it becomes almost stable. The mean difference between the values of E evaluated with the aid of analytical Equation (25) and those determined from the FEA by Equation (13) are 0.306%, 0.461%, 0.531%, 0.308% for SWBNNTs, SWBPNTs, SWBAsNTs and SWBSbNTs, respectively, which shows that equation (25) allows calculating accurately the Young's modulus of the B – A15 nanotubes regardless their chirality, diameter and compound, forming nanotube, without resorting to numerical simulation.

The Young's moduli for zigzag, E_x, and armchair, E_y, configurations of the B-A15 nanosheets, derived from the FEA and calculated using equations (18) and (19), respectively, are also plotted in Figure 4.3. It can be noticed that the values of the Young's moduli for the B – A15 nanosheets are practically equal to the values obtained from the FEA and calculated by equation (25), for diameters $D_n > 2.5$ nm.

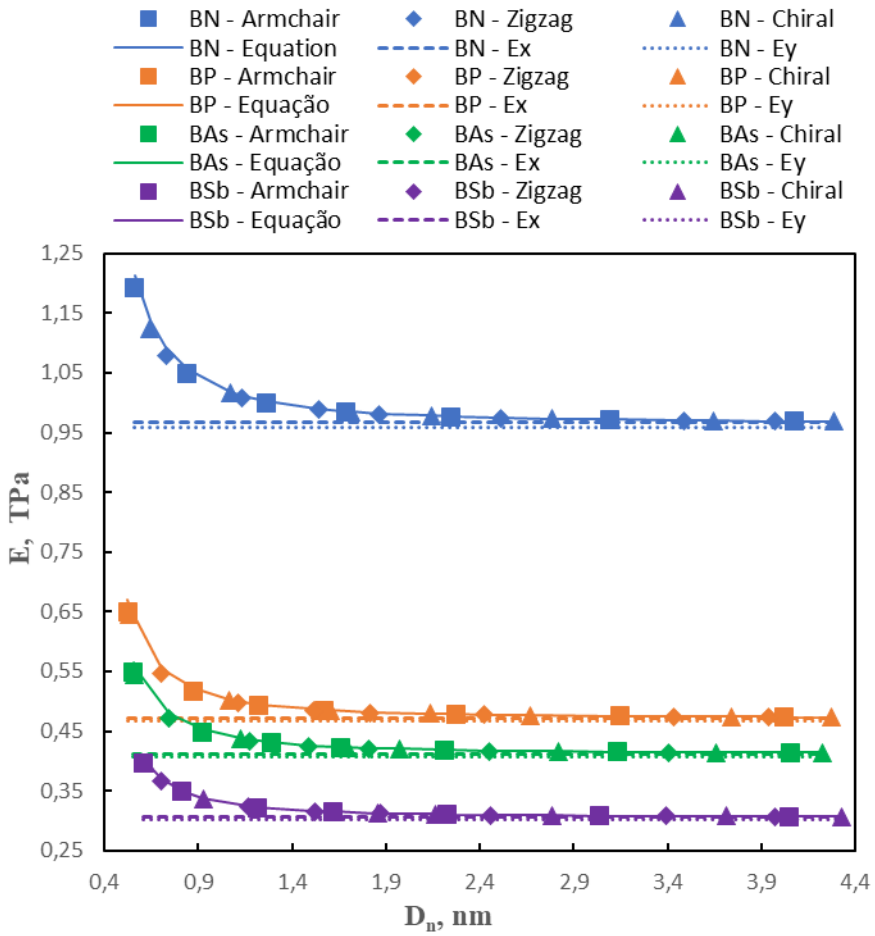

Figure 4.3. Evolution of the Young's modulus, E, with the nanotube diameter, D_n, for B – A15 nanotubes and nanosheets.

Similarly, Figure 4.4 shows the evolution of the shear modulus, G, with the nanotube diameter, D_n, as well as the values calculated by equation (26). In this case, the shear modulus, becomes almost stable after the nanotube diameter reaches $D_n > 0.9$ nm, regardless compound or nanotube chirality. The mean difference between the values of G evaluated with the aid of analytical equation (26) and those determined from the FEA by Equation (14) are 1.003%, 2.153%, 2.503%, 2.807%, for SWBNNTs, SWBPNTs, SWBAsNTs and SWBSbNTs, respectively. While these values are relatively low, they can be further improved by considering only values where the shear modulus is stabilized, for the nanotube diameters $D_n > 0.9$ nm. In this case the mean difference values decrease to 0.293%, 0.597%, 1.128%, 0.930%, for SWBNNTs, SWBPNTs, SWBAsNTs and SWBSbNTs, respectively, which demonstrates that equation (26) allows calculating the shear modulus of the B – A15 nanotubes, regardless their chirality and constituent

compound, without resorting to the numerical simulation, with even greater accuracy in the stable range, for diameters $D_n > 0.9$ nm.

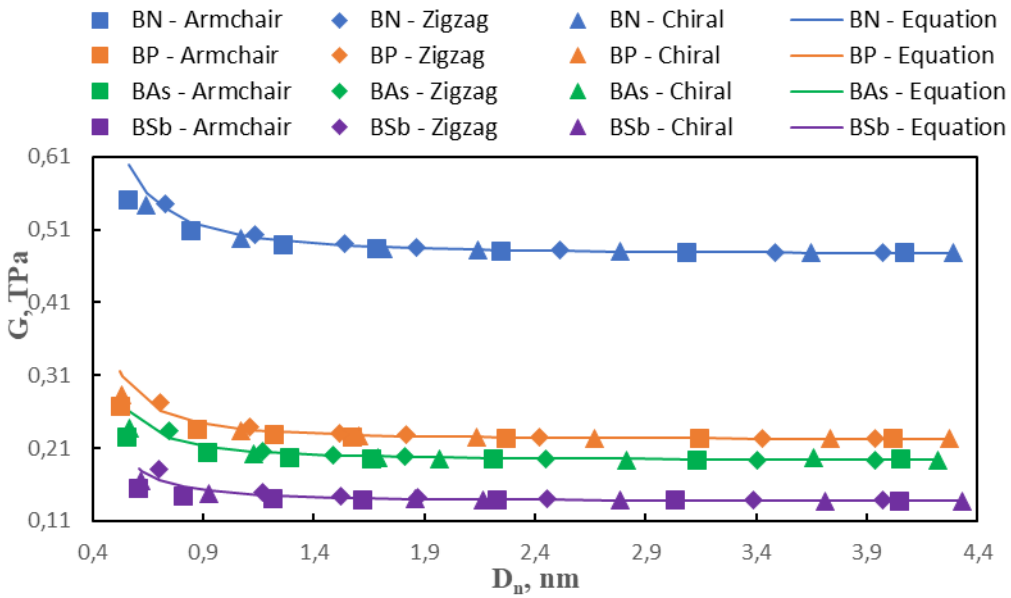

Figure 4.4. Evolution of the shear modulus, G, with the nanotube diameter, D_n, for B – A15 nanotubes.

Figure 4.5a shows the evolution of the Poisson's ratio, ν, with the nanotube diameter, D_n, as well as the values calculated by equation (27), which does not depend on the nanotube diameter, D_n. The Poisson's ratio converges to the value given by equation (27), when the nanotube diameter, D_n becomes high enough. As the bond length, a_{B-A15}, increases, the nanotube diameter, D_n, for which a stable Poisson's ratio, ν, value is achieved, also increases. The stable nanotube diameter values are approximately 2.0, 2.1, 2.4, 2.7 for SWBNNTs, SWBPNTs, SWBAsNTs and SWBSbNTs, respectively, where the mean difference between the values of ν evaluated with the aid of analytical equation (27) and those determined from the FEA by Equation (15), in the stable range, for the NTs with $D_n > 2.2$ nm, are 1.178%, 0.541%, 2.856%, 0.115%, for SWBNNTs, SWBPNTs, SWBAsNTs and SWBSbNTs, respectively. This demonstrates that equation (27) allows accurate assessment of the Poisson's ratio, ν, of the B – A15 nanotubes with the diameters higher than 2.2 nm, regardless their chirality and forming compound, without resorting to numerical simulation. For cases where the nanotube diameter is lower than 2.2 nm, the Poisson's ratio, ν, decreases for armchair and chiral NTs and increases for zigzag NTs.

To understand the effect of the 15th group element (N, P, As, Sb) on the nanotube's Poisson's ratio , the ν values obtained by equation (27) are shown in Figure 4.5b as a function of bond length, a_{B-A15}. As Figure 4.5b shows when the value of bond length, a_{B-A15}, increases, the of Poisson's ratio, ν, increases as well.

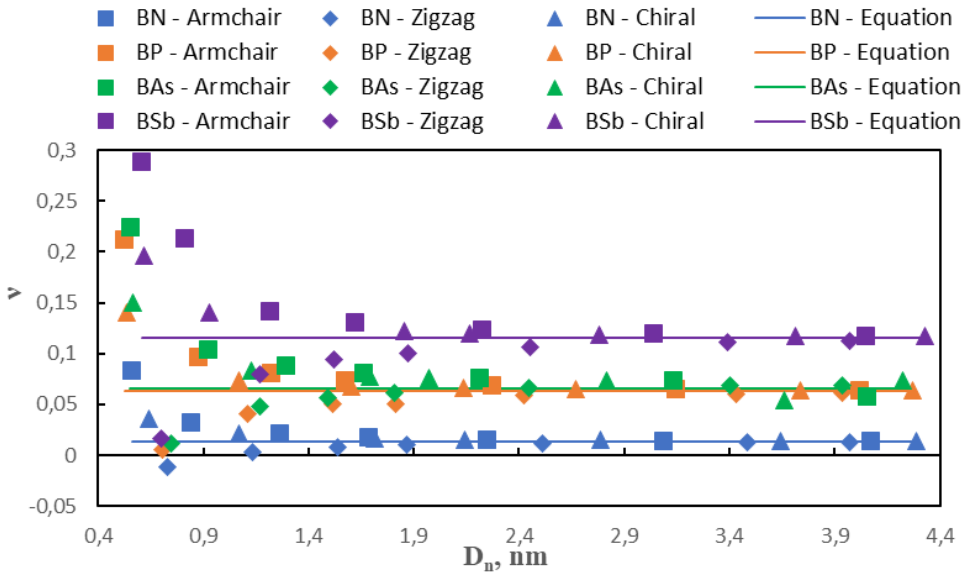

(a)

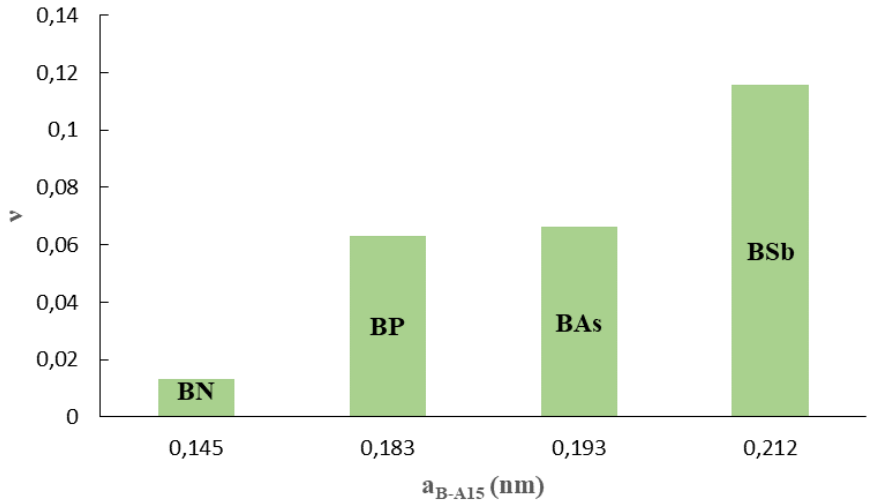

(b)

Figure 4.5. Evolution of the Poisson's ratio, ν, for B – A15 nanotubes as a function of (a) nanotube diameter, D_n, and (b) bond length, a_{B-A15}.

To facilitate comparison, the results of the Young's, E, and shear, G, moduli and Poisson's ratio, ν, for the B – A15 nanotubes, calculated using equations (25)-(27) are presented in Table 4.2.

Table 4.2. Young's and shear moduli, and Poisson's ratio of SWBNNTs, SWBPNTs, SWBAsNTs, SWBSbNTs.

Compound	Elastic Properties*		
	E, TPa	G, TPa	ν
BN	0.971	0.479	0.013
BP	0.475	0.223	0.063
BAs	0.416	0.195	0.066
BSb	0.308	0.138	0.116

*Converged mean values.

4.3. Surface Elastic Moduli

In a similar way to what was done in the previous section, the surface Young's and shear moduli of the B – A15 nanotubes were initially evaluated using equations (16) and (17), which utilized the tensile, bending and torsional results obtained by FEA. However, by utilizing the fitting parameters α_{B-A15}, β_{B-A15}, and γ_{B-A15}, presented in Table 4.1, and relating equations (16) and (17) with equations (22)-(24), new analytical expressions can be obtained that are independent of nanotube diameter, D_n, or wall thickness, t_n. These expressions allow the direct calculation of the surface Young's and shear moduli without resorting to the FEA results, respectively, as follows [16]:

$$E_s = \frac{\alpha_{B-A15}}{\pi\sqrt{8\left(\frac{\beta_{B-A15}}{\alpha_{B-A15}}\right)}} \tag{28}$$

$$G_s = \frac{\gamma_{B-A15}}{\pi\sqrt{32\left(\frac{\beta_{B-A15}}{\alpha_{B-A15}}\right)^3}} \tag{29}$$

Figure 4.6a displays the evolution of the surface Young's modulus, E_s, with the nanotube diameter, D_n, as well the values calculated by equation (28). Regardless compound or chirality, the surface Young's modulus is nearly constant in the whole range of D_n, considered in this dissertation. The mean difference between E_s values assessed by equation (17) and those calculated by equation (28) are 0.249%, 0.344%, 0.397%, 0.366%, for

SWBNNTs, SWBPNTs, SWBAsNTs, SWBSbNTs, respectively, which shows that equation (28) allows calculating the surface Young's modulus of the B – A15 nanotubes without resorting to numerical simulation, regardless their chirality and diameter.

The surface Young's moduli, E_{sx} (zigzag configuration), and E_{sy} (armchair configuration), of the B-A15 nanosheets, derived from the FEA results and calculated using equations (20) and (21), respectively, are also plotted in Figure 4.6a. It is worth noting, the values of E_S of single-walled B – A 15 nanotubes are nearly equal to E_{sx} obtained for zigzag configuration and slightly higher than the E_{sy} value for armchair configuration of the respective nanosheet.

To understand the effect of the 15th group element (N, P, As, Sb) on the nanotube's surface Young's modulus, E_S, the values obtained by equation (28) are shown in Figure 4.6b as a function of bond length, a_{B-A15}. As Figure 4.6b shows as the values of bond length, a_{B-A15}, increases, the values of surface Young's modulus, E_s, decrease.

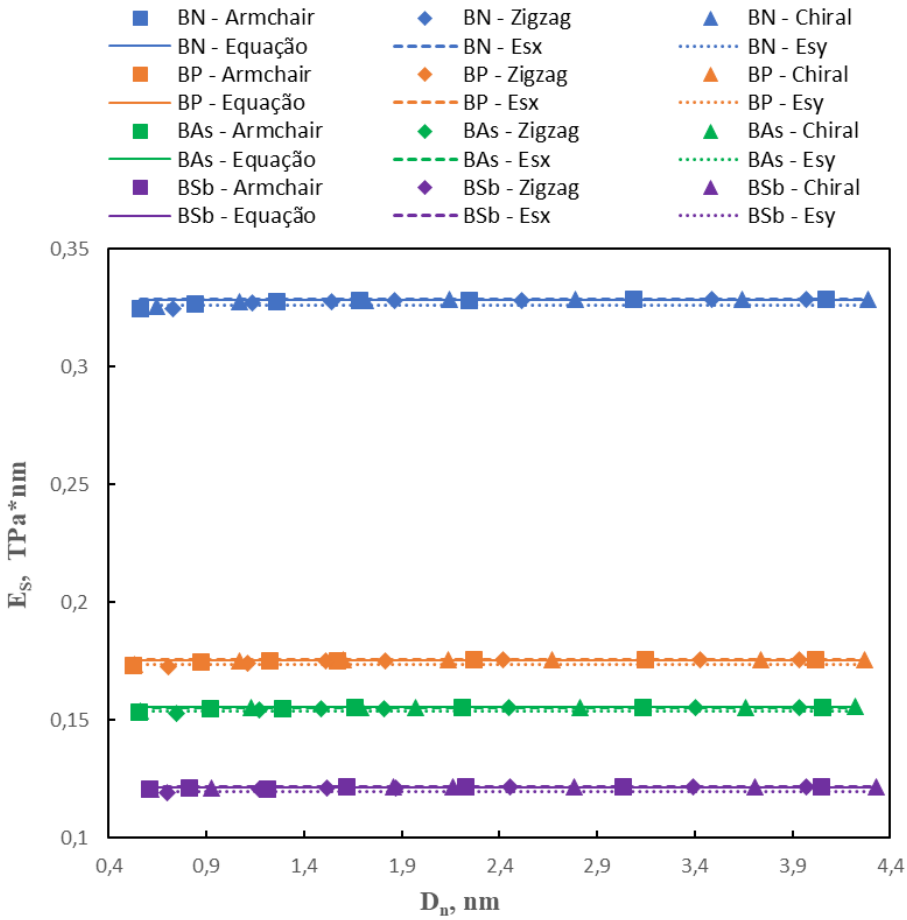

(a)

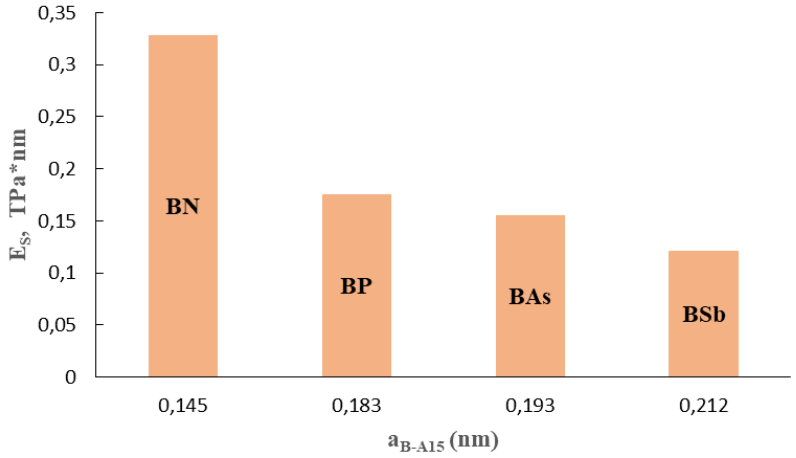

(b)

Figure 4.6. Evolution of the surface Young's modulus, E_s, for B – A15 nanotubes and nanosheets as a function of (a) nanotube diameter, D_n, and (b) bond length, $a_{B\text{-}A15}$.

Similarly, Figure 4.7a shows the evolution of the surface shear modulus, G_s, with the nanotube diameter, D_n, as well as the values calculated by equation (29). In this case, the surface shear modulus, becomes almost stable after it reaches diameters $D_n > 1.4$ nm, regardless of compound or chirality. The mean difference between G_s values assessed by equation (18) and those calculated by equation (29) are 0.935%, 1.978%, 2.327%, 2.674%, for SWBNNTs, SWBPNTs, SWBAsNTs and SWBSbNTs, respectively. While these values are relatively low, they can be further improved by considering only values where the surface shear modulus has stabilized for the nanotube diameters $D_n > 1.4$ nm. In this case the mean difference values decrease to 0.172%, 0.379%, 0.743%, 0.531%, for SWBNNTs, SWBPNTs, SWBAsNTs and SWBSbNTs, respectively, which demonstrates that equation (29) allows calculating the shear modulus of B – A15 nanotubes, regardless of chirality and diameter, without resorting to numerical simulation, with even greater accuracy in the stable range, for diameters $D_n > 1.4$ nm.

To understand the effect of the 15th group element (N, P, As, Sb) on the nanotube's surface shear modulus, G_s, the values obtained by equation (29) are shown in Figure 4.7b as a function of the bond length, a_{B-A15}. As Figure 4.7b shows as the values of bond length, a_{B-A15}, increases, the values of surface shear modulus, G_s, decrease.

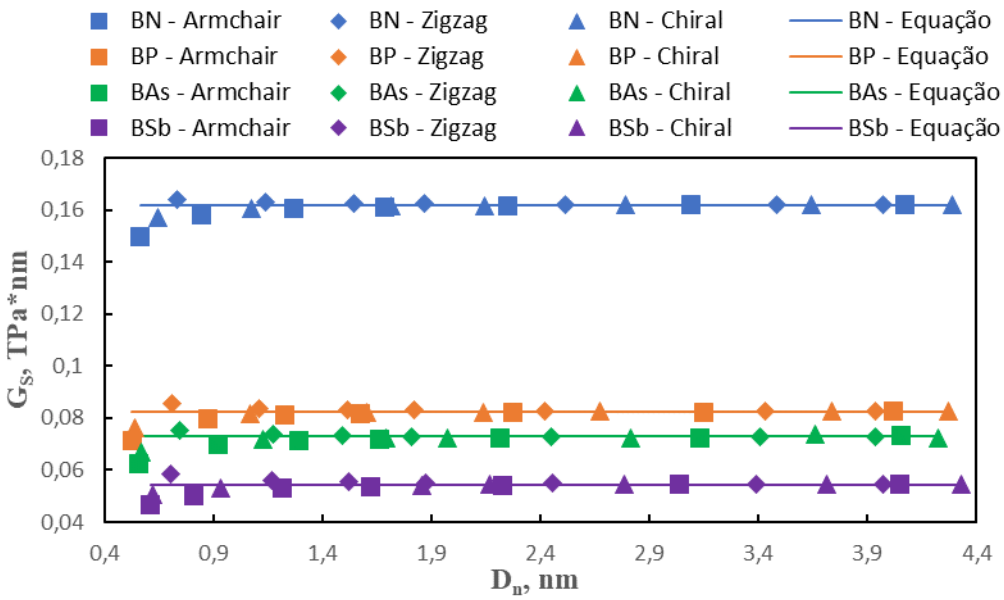

(a)

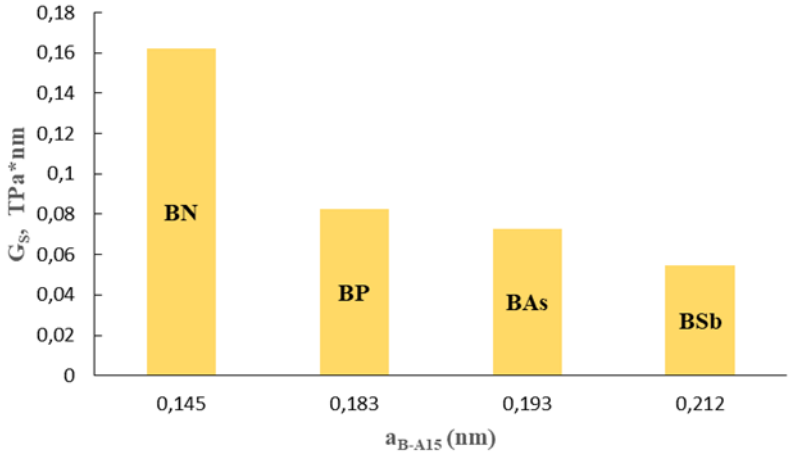

(b)

Figure 4.7. Evolution of the surface shear modulus, G_s, for B – A15 nanotubes as a function of (a) nanotube diameter, D_n, and (b) bond length, $a_{B\text{-}A15}$.

To enable an easier comparison, the results of the surface Young's, E_s, and shear, G_s, moduli for the B – A15 nanotubes, calculated using equations (28) and (29) are presented in Table 4.3.

Table 4.3. Surface Young's and shear moduli of SWBNNTs, SWBPNTs, SWBAsNTs, SWBSbNTs.

Compound	Elastic Properties	
	E_S, TPa*nm	**G_S, TPa*nm**
BN	0.328	0.162
BP	0.175	0.083
BAs	0.155	0.073
BSb	0.122	0.054

It is worth noting that the elastic moduli values calculated in this dissertation for the SWBNNTs and SWBPNTs are similar to those reported in the works of Sakharova et al.[7], [15]. In these studies, comprehensive comparison with existent literature results was carried out and showed that the present modelling approach leads to accurate evaluation of the mechanical properties of the abovementioned nanotubes.

5. CONCLUSIONS AND FUTURE PERSPECTIVES

In summary, this dissertation aimed to realize a numerical simulation study based on the NCM/MSM approach that allowed the evaluation of the elastic properties, namely, the tensile, bending and torsional rigidities, the Young's and shear moduli, the surface Young's and shear moduli, and the Poisson's ratio of the SWBNNTs, SWBPNTs, SWBAsNTs and SWBSbNTs as well respective nanosheets.

Using the FEA results it was possible to obtain analytical expressions that enabled the evaluation of the three rigidities as a function of the nanotube diameter, knowing the fitting parameters, without resorting to numerical simulation for the single-walled nanotubes formed by the boron compounds.

With the knowledge of the fitting parameters, analytical expressions were used to obtain the Young's and shear moduli, Poisson's ratio and the surface Young's and shear moduli of the B – A15 nanotubes, without resourcing to the numerical simulation. These analytical relationships permit accurate evaluation of the Young´s moduli within the whole range of the nanotube diameters considered. While for the shear moduli and the Poisson´s ratio such precise assessment is possible for the nanotube diameters domain where these elastic properties become stable.

The tensile, bending and torsional rigidities, the Young's and shear moduli, the surface Young's and shear moduli, and the Poisson's ratio of SWBNNTs, SWBPNTs, SWBAsNTs and SWBSbNTs and respective nanosheets are influenced by the bond length, $a_{\mathrm{B-A15}}$. With increasing of the bond length all elastic properties under consideration decrease with the exception of the Poisson's ratio which increases.

The present results constitute a considerable contribution to a reference regarding the determination of the elastic properties of boron compounds-based nanotubes by theoretical methods.

In view of modern requirements for the search of new materials for innovative nanodevices, the future studies will be focused on the investigation of the elastic properties of other non-carbon nanotubes. Amongst them, the nanotubes from compounds formed by the other elements of the 13th group, such as aluminium (Al), gallium (Ga) and indium (In), with the elements of the 15th group (N, P, As, Sb), are of particular research interest.

REFERENCES

[1] D. Golberg, Y. Bando, Y. Huang, T. Terao, M. Mitome, C. Tang, C. Zhi, 'Boron Nitride Nanotubes and Nanosheets', *ACS Nano*, 2010, 4, 6, 2979–2993, doi: 10.1021/nn1006495.

[2] X. Dai, X. Zhang, and H. Li, 'Semiconductor-metal transition in multi-layer sandwiched BAs/BP heterostructures induced by BP intercalation', *Appl Surf Sci*, vol. 507, Mar. 2020, doi: 10.1016/j.apsusc.2019.144923.

[3] X. Dai, Y. Jiang, and H. Li, 'BAs nanotubes with non-circular cross section shapes for gas sensors', *Physical Chemistry Chemical Physics*, vol. 22, no. 22, pp. 12584–12590, Jun. 2020, doi: 10.1039/d0cp01708f.

[4] C. Li and T. W. Chou, 'Static and Dynamic Properties of Single-Walled Boron Nitride Nanotubes', *J Nanosci Nanotechnol*, vol. 6, no. 1, pp. 54–60, 2006, doi: 10.1166/JNN.2006.17904.

[5] M. Salavati, H. Ghasemi, and T. Rabczuk, 'Electromechanical properties of Boron Nitride Nanotube: Atomistic bond potential and equivalent mechanical energy approach', *Comput Mater Sci*, vol. 149, pp. 460–465, Jun. 2018, doi: 10.1016/J.COMMATSCI.2018.03.037.

[6] R. Ansari, M. Mirnezhad, and S. Sahmani, 'Prediction of chirality- and size-dependent elastic properties of single-walled boron nitride nanotubes based on an accurate molecular mechanics model', *Superlattices Microstruct*, vol. 80, pp. 196–205, Apr. 2015, doi: 10.1016/J.SPMI.2014.12.033.

[7] N. A. Sakharova, J. M. Antunes, A. F. G. Pereira, B. M. Chaparro, and J. V. Fernandes, 'On the determination of elastic properties of single-walled boron nitride nanotubes by numerical simulation', *Materials*, vol. 14, no. 12, Jun. 2021, doi: 10.3390/ma14123183.

[8] J. W. Yan and K. M. Liew, 'Predicting elastic properties of single-walled boron nitride nanotubes and nanocones using an atomistic-continuum approach', *Compos Struct*, vol. 125, pp. 489–498, Jul. 2015, doi: 10.1016/J.COMPSTRUCT.2015.02.043.

[9] A. Genoese, A. Genoese, and G. Salerno, 'On the nanoscale behaviour of single-wall C, BN and SiC nanotubes', *Acta Mech*, vol. 230, no. 3, pp. 1105–1128, Mar. 2019, doi: 10.1007/S00707-018-2336-7/METRICS.

[10] L. Jiang and W. Guo, 'Analytical solutions for elastic binary nanotubes of arbitrary chirality', *Acta Mechanica Sinica 2016 32:6*, vol. 32, no. 6, pp. 1046–1057, Sep. 2016, doi: 10.1007/S10409-016-0581-3.

[11] A. K. Rappé, C. J. Casewit, K. S. Colwell, W. A. Goddard, and W. M. Skiff, 'UFF, a Full Periodic Table Force Field for Molecular Mechanics and Molecular Dynamics Simulations', *J Am Chem Soc*, vol. 114, no. 25, pp. 10024–10035, Dec. 1992, doi: 10.1021/JA00051A040/SUPPL_FILE/JA00051A040_SI_001.PDF.

[12] S. L. Mayo, B. D. Olafson, and W. A. Goddard, 'DREIDING: A generic force field for molecular simulations', *Journal of Physical Chemistry*, vol. 94, no. 26, pp. 8897–8909, 1990, doi: 10.1021/J100389A010/ASSET/J100389A010.FP.PNG_V03.

[13] L. Jiang and W. Guo, 'A molecular mechanics study on size-dependent elastic properties of single-walled boron nitride nanotubes', *J Mech Phys Solids*, vol. 59, no. 6, pp. 1204–1213, Jun. 2011, doi: 10.1016/J.JMPS.2011.03.008.

[14] J. W. Yan, J. B. He, and L. H. Tong, 'Longitudinal and Torsional Vibration Characteristics of Boron Nitride Nanotubes', *Journal of Vibration Engineering & Technologies 2019 7:3*, vol. 7, no. 3, pp. 205–215, May 2019, doi: 10.1007/S42417-019-00113-4.

[15] N. A. Sakharova, J. M. Antunes, A. F. G. Pereira, B. M. Chaparro, and J. V. Fernandes, 'Elastic Properties of Single-Walled Phosphide Nanotubes: Numerical Simulation Study', *Nanomaterials*, vol. 12, no. 14, Jul. 2022, doi: 10.3390/nano12142360.

[16] N. A. Sakharova, A. F. G. Pereira, J. M. Antunes, B. M. Chaparro, T. G. Parreira, and J. V. Fernandes, 'On the Determination of Elastic Properties of Single-Walled Nitride Nanotubes Using Numerical Simulation', *Materials*, vol. 17, no. 10, p. 2444, May 2024, doi: 10.3390/ma17102444.

[17] H. S. Şahin *et al.*, 'Monolayer honeycomb structures of group IV elements and III-V binary compounds', *Phys Rev*, 2009.

[18] L.-C. Qin, 'Determination of the chiral indices (n, m) of carbon nanotubes by electron diffraction', *Phys Chem Chem Phys*, 2007, 9, 31-48, doi: 10.1039/b614121h.

[19] A. L. Kalamkarov, A. V. Georgiades, S. K. Rokkam, V. P. Veedu, and M. N. Ghasemi-Nejhad, 'Analytical and numerical techniques to predict carbon nanotubes properties', *Int J Solids Struct*, vol. 43, no. 22–23, pp. 6832–6854, Nov. 2006, doi: 10.1016/J.IJSOLSTR.2006.02.009.

[20] Eduardo B. Barros, Ado Jorio, Georgii G. Samsonidze, Rodrigo B. Capaz, Antônio G. Souza Filho, Josué Mendes Filho, Gene Dresselhaus, Mildred S. Dresselhaus, Review on the symmetry-related properties of carbon nanotubes, Physics Reports, Volume 431, Issue 6, 2006, Pages 261-302, https://doi.org/10.1016/j.physrep.2006.05.007.

[21] J. M. Antunes, A. F. G. Pereira, and N. A. Sakharova, 'Overview on the Evaluation of the Elastic Properties of Non-Carbon Nanotubes by Theoretical Approaches', May 01, 2022, *Materials*. doi: 10.3390/ma15093325.

[22] C. Li and T.-W. Chou, 'A structural mechanics approach for the analysis of carbon nanotubes', *Int J Solids Struct*, 2003, *40*, 2487–2499, doi: 10.1016/S0020-7683(03)00056-8.

[23] N. A. Sakharova, A. F. G. Pereira, J. M. Antunes, C. M. A. Brett, and J. V. Fernandes, 'Mechanical characterization of single-walled carbon nanotubes: Numerical simulation study', *Compos B Eng*, vol. 75, pp. 73–85, Jun. 2015, doi: 10.1016/J.COMPOSITESB.2015.01.014.

[24] A. F. G. Pereira, J. V. Fernandes, J. M. Antunes, and N. A. Sakharova, 'Shear modulus and Poisson's ratio of single-walled carbon nanotubes: Numerical evaluation', *Phys Status Solidi B Basic Res*, vol. 253, no. 2, pp. 366–376, Feb. 2016, doi: 10.1002/PSSB.201552320.

[25] P. Hess, 'Thickness of elemental and binary single atomic monolayers', *Nanoscale Horiz*, vol. 5, no. 3, pp. 385–399, Mar. 2020, doi: 10.1039/C9NH00658C.

[26] N. A. Sakharova, J. M. Antunes, A. F. G. Pereira, B. M. Chaparro, T. G. Parreira, and J. V. Fernandes, 'Numerical Evaluation of the Elastic Moduli of AlN and GaN Nanosheets', *Materials*, vol. 17, no. 4, Feb. 2024, doi: 10.3390/ma17040799.

[27] N. A. Sakharova, A. F. G. Pereira, and J. M. Antunes, 'Elastic Moduli of Non-Chiral Singe-Walled Silicon Carbide Nanotubes: Numerical Simulation Study', *Materials*, vol. 15, no. 22, Nov. 2022, doi: 10.3390/ma15228153.

[28] J. V. Fernandes, A. F. G. Pereira, J. M. Antunes, B. M. Chaparro, and N. A. Sakharova, 'Numerical Simulation Study of the Mechanical Behaviour of 1D and 2D Germanium Carbide and Tin Carbide Nanostructures', *Materials 2023, Vol. 16, Page 5484*, vol. 16, no. 15, p. 5484, Aug. 2023, doi: 10.3390/MA16155484.